Since January 2020 Elsevier has created a COVID-19 resource centre with free information in English and Mandarin on the novel coronavirus COVID-19. The COVID-19 resource centre is hosted on Elsevier Connect, the company's public news and information website.

Elsevier hereby grants permission to make all its COVID-19-related research that is available on the COVID-19 resource centre - including this research content - immediately available in PubMed Central and other publicly funded repositories, such as the WHO COVID database with rights for unrestricted research re-use and analyses in any form or by any means with acknowledgement of the original source. These permissions are granted for free by Elsevier for as long as the COVID-19 resource centre remains active.

Virology 565 (2022) 96–105

Contents lists available at ScienceDirect

Virology

journal homepage: www.elsevier.com/locate/virology

Swine acute diarrhea syndrome coronavirus replication is reduced by inhibition of the extracellular signal-regulated kinase (ERK) signaling pathway

Jiyu Zhang [1], Liaoyuan Zhang [1], Hongyan Shi, Shufeng Feng, Tingshuai Feng, Jianfei Chen, Xin Zhang, Yuru Han, Jianbo Liu, Yiming Wang, Zhaoyang Ji, Zhaoyang Jing, Dakai Liu, Da Shi [**], Li Feng [*]

State Key Laboratory of Veterinary Biotechnology, Harbin Veterinary Research Institute, Chinese Academy of Agricultural Sciences, Xiangfang District, Haping Road 678, Harbin, 150069, China

ARTICLE INFO

Keywords:
Swine acute diarrhea syndrome coronavirus (SADS-CoV)
ERK pathway
Viral replication
Apoptosis

ABSTRACT

Swine acute diarrhea syndrome coronavirus (SADS-CoV) is a newly discovered enteric coronavirus. We have previously shown that the caspase-dependent FASL-mediated and mitochondrion-mediated apoptotic pathways play a central role in SADS-CoV-induced apoptosis, which facilitates viral replication. However, the roles of intracellular signaling pathways in SADS-CoV-mediated cell apoptosis and the relative advantages that such pathways confer on the host or virus remain largely unknown. In this study, we show that SADS-CoV induces the activation of ERK during infection, irrespective of viral biosynthesis. The knockdown or chemical inhibition of ERK1/2 significantly suppressed viral protein expression and viral progeny production. The inhibition of ERK activation also circumvented SADS-CoV-induced apoptosis. Taken together, these data suggest that ERK activation is important for SADS-CoV replication, and contributes to the virus-mediated changes in host cells. Our findings demonstrate the takeover of a particular host signaling mechanism by SADS-CoV and identify a potential approach to inhibiting viral spread.

1. Introduction

Coronaviruses, categorized in the order *Nidovirales*, family *Coronaviridae*, and subfamily *Coronavirinae*, are a large group of viral pathogens with a wide host range (Cui et al., 2019). Their infection of humans, other mammals, and birds can cause enteric, respiratory, neurological, and hepatic diseases with varying severity (Fehr and Perlman, 2015). In the past two decades, coronaviruses have become a serious threat to humans, causing major epidemics and pandemics, including SARS in 2003, Middle East respiratory syndrome (MERS) in 2012, and COVID-19 in 2020.

In addition to the threat they pose to humans, coronaviruses such as swine acute diarrhea syndrome coronavirus (SADS-CoV) infect domestic animals and impose substantial economic losses. SADS-CoV (also known as SeACoV or PEAV) is a newly identified coronavirus that causes severe acute diarrhea and rapid weight loss in piglets less than 6 days old. SADS-CoV is most closely related to bat coronavirus HKU2, although it is also distantly related to other coronaviruses, including HCoV 229E, HCoV NL63, and the swine coronavirus PEDV (Gong et al., 2017). *Rhinolophus* bat species carrying the bat virus HKU2, which shares high sequence similarity with SADS-CoV strains, have been observed in the vicinity of local outbreaks, suggesting that SADS-CoV probably originated in bats (Zhou et al., 2018). SADS-CoV induces apoptosis both in cultured cells and in target tissues *in vivo*, and cell apoptosis has been shown to play a major role in the pathophysiology of SADS-CoV infection (Zhang et al., 2020).

Among the first host responses induced by viral infection are the cell autonomous immune responses. These functions are ubiquitous to every cell type and are normally triggered by pattern recognition receptors, which detect various components of the incoming pathogen (Bieniasz,

* Corresponding author. Harbin Veterinary Research Institute, CAAS, 678 Haping Road Xiangfang District, Harbin, 150069, China.
** Corresponding author. Harbin Veterinary Research Institute, CAAS, 678 Haping Road Xiangfang District, Harbin, 150069, China.
E-mail addresses: shida@caas.cn (D. Shi), fengli@caas.cn (L. Feng).
[1] These authors contributed equally to this work.

https://doi.org/10.1016/j.virol.2021.10.009
Received 25 August 2021; Received in revised form 25 October 2021; Accepted 26 October 2021
Available online 30 October 2021
0042-6822/© 2021 Elsevier Inc. All rights reserved.

2004; Everett and Chelbi-Alix, 2007; Randow et al., 2013). Mitogen-activated protein kinases (MAPKs) are a family of serine–-threonine protein kinases that, as well as being important mediators of signal transduction from the cell surface to the nucleus, are thought to play important roles in the initiation and progression of cell death (Cohen, 1997). MAPKs constitute a superfamily of highly related serine–threonine kinases. At least seven members of the MAPK family have been identified in mammals: the extracellular signal-regulated kinases ERK1 and ERK 2 (ERK1/2) (Blenis, 1993; Lange-Carter et al., 1993), c-Jun NH_2-terminal kinase (JNK)/stress-activated protein kinase (Blenis, 1993; Lange-Carter et al., 1993), p38 MAPK (Blenis, 1993) (Lange-Carter et al., 1993), big MAPK1 (BMK1) (Lee et al., 1995), ERK6 (Lechner et al., 1996), and ERK7 (Abe et al., 1999). Each MAPK pathway generally consists of three kinase modules: a MAPK, a MAPK kinase (MAPKK), and a MAPKK kinase (MAPKKK). These kinase modules are differentially activated by a variety of cellular stimuli and contribute to distinct cellular functions. It is assumed that the commitment of a cell to apoptosis involves a balance between the activities of ERK, JNK, and p38 MAPK. The ERK signaling pathway includes RAF, MEK 1 and MEK2 (MEK1/2), and ERK1/2, and plays important roles in the regulation of cell survival, proliferation, and differentiation (Roux and Blenis, 2004).

Because viruses are obligate intracellular parasites, they have developed the ability to manipulate a variety of host-cell signal transduction pathways, including the ERK pathway, to benefit their own multiplication. Many viruses have been shown to exploit the ERK pathway for maximal viral replication and gene expression (Jeon et al., 2020; Kim and Lee, 2015; Lee and Lee, 2010). However, the intracellular signaling mechanisms involved in SADS-CoV replication were unknown. Therefore, in this study, we investigated the role of the ERK pathway in SADS-CoV infection. We found that SADS-CoV induces the early, strong and transient activation of ERK, independently of maximal viral gene expression. Furthermore, the ultraviolet (UV)-inactivated virus was sufficient to trigger ERK activation, indicating a critical role for the viral entry process in ERK phosphorylation. The treatment of cells with the ERK1/2 inhibitor U0126 or PD98059 significantly inhibited SADS-CoV infection. Our experimental results showed that the inhibition of ERK activation significantly reduced viral protein expression and the release of viral progeny. Further experiments revealed that the inhibition of ERK activities correlated with a reduction in the apoptosis of SADS-CoV-infected cells. Together, these data indicate a pivotal role for the ERK signaling pathway in the SADS-CoV life cycle.

2. Material and methods

2.1. Cells, viruses, reagents, and antibodies

Vero E6 and IPI-2I cells (porcine intestinal epithelial cells) were cultured in Dulbecco's minimal essential medium (DMEM; Sigma-Aldrich, St Louis, USA) with 10% fetal bovine serum (FBS; Invitrogen, USA) and antibiotic–antimycotic solution (100 × ; Invitrogen). The cells were maintained at 37 °C in a humidified incubator under 5% CO_2. SADS-CoV (GenBank accession No. MF094681) was isolated from the intestinal-tract contents of SADS-CoV-infected piglets in Guangdong Province, China, and identified with physicochemical and neutralization testing and reverse transcription (RT)–PCR and DNA sequencing analyses (Zhou et al., 2018). The viral and mock inoculum stocks were prepared by freezing/thawing virus-infected or mock-infected Vero E6 cells, respectively. SADS-CoV was inactivated with UV irradiation (1000 mJ/cm^2) of a viral suspension with a UV crosslinker (Stratagene). Virus inactivation was confirmed by the inoculation of Vero E6 cells with the UV-treated virus, followed by N-protein-specific staining, as described below, and the inactivated virus was stored at −80 °C. U0126 and PD98059 were obtained from Cell Signaling Technology (Danvers, USA). SADS-CoV N-protein-specific monoclonal antibody was prepared in our laboratory (Han et al., 2019). Antibodies specific for phosphorylated ERK1/2 (p-ERK1/2), ERK1/2, p-ELK1, poly (ADP-ribose) polymerase (PARP), proliferating cell nuclear antigen (PCNA), and glyceraldehyde 3-phosphate dehydrogenase (GAPDH) were all obtained from Abcam.

2.2. Western blotting analyses

Target cells grown to confluence in six-well tissue culture plates were serum starved for 24 h before infected with SADS-CoV or UV-SADS-CoV at 37 °C. At the indicated times, cells were harvested in 200 μL of RIPA buffer (Sigma-Aldrich, St Louis, USA) and sonicated on ice 5 times for 1 s each. Homogenates were lysed for 30 min on ice, and clarified by centrifugation at 15,000 g for 20 min at 4 °C. To examine the effect of ERK inhibition on SADS-CoV replication, cells were pretreated independently with each MEK inhibitor for 1 h and then infected with SADS-CoV at an MOI of 0.1. The virus-inoculated cells were further propagated in the presence of U0126, PD98059, or DMSO and cell lysates were prepared with RIPA buffer at 36 h. Proteins separated with 12.5% sodium dodecyl sulfate polyacrylamide gel electrophoresis (SDS-PAGE) were electroblotted onto 0.45 μm reinforced nitrocellulose membranes in transfer buffer (0.5 mM Tris-HCl, 0.2 M glycine, 20% methanol) at 300 mA for 180 min with a Mini Trans-Blot Electrophoretic Transfer Cell (Bio-Rad). The membranes were blocked with 5% (w/v) skim milk in phosphate-buffered saline (PBS) overnight at 4 °C and then hybridized with the primary antibody in TBST (20 mM Tris-HCl [pH 7.5], 150 mM NaCl, 0.05% Tween 20) for 2 h. After the membranes were rinsed five times with TBST, they were transferred to TBST containing IRDye-800CW-conjugated goat anti-mouse lgG (H + L) antibody (LiCor BioSciences) or IRDye-680RD-conjugated goat anti-rabbit lgG (H + L) antibody (LiCor BioSciences), and the blots were then visualized with the Odyssey Infrared Imaging System (LiCor BioSciences). The band intensities were quantified with densitometry using the ImageJ software (NIH, Maryland, USA).

2.3. Immunofluorescence assay

Vero E6 cells were cultured in glass-bottomed dishes (MatTek) or in six-well tissue culture plates. The cells were fixed with 4% paraformaldehyde for 30 min and permeabilized with 1% Triton X-100 for 15 min at room temperature for intracellular labeling. They were then incubated with the primary antibody for 2 h at room temperature. When a secondary antibody was required, the cells were incubated with the corresponding Alexa-Fluor-conjugated secondary antibody (Invitrogen) for 1 h at room temperature, and then counterstained with 4′,6-diamidino-2-phenylindole (DAPI; Sigma, USA) at room temperature for 15 min. Images were captured with an inverted fluorescent microscope (Zeiss, Munich, Germany) or LSM 800 confocal microscope (Zeiss) using oil immersion objective. The red-fluorescence-positive cells were quantified by averaging at least six fields of view.

2.4. Nuclear and cytoplasmic protein extraction

Nuclear and cytoplasmic cell fractions were prepared with an NE-PER Nuclear and Cytoplasmic Extraction Reagents (Thermo Scientific, USA) according to the manufacturer's instructions. Briefly, the treated Vero E6 cells were scraped into ice-cold PBS and centrifuged at 500×*g* for 3 min. The cell pellet was suspended in 300 μL of ice-cold CER I with vortexing. The suspension was incubated on ice for 10 min, and 16.5 μL of ice-cold CER II was added. The sample was vortexed for 5 s, incubated on ice for 1 min, and centrifuged for 5 min at maximum speed. The supernatant fraction (cytoplasmic extract) was transferred to a pre-chilled tube and used as the cytoplasmic fraction. The insoluble pellet fraction, which contained crude nuclei, was resuspended in 150 μL of ice-cold NER with vortexing for 15 s, incubated on ice for 10 min, and then centrifuged for 10 min at maximum speed. The resulting supernatant, constituting the nuclear extract, was used in subsequent experiments. To ensure that the subcellular fractions were properly separated,

the subcellular lysates were verified with antibodies directed against the corresponding fractions: anti-glyceraldehyde 3-phosphate dehydrogenase (anti-GAPDH) antibody for the cytoplasmic fraction and anti-proliferating cell nuclear antigen (anti-PCNA) antibody for the nuclear fraction.

2.5. Knockdown of ERK expression with siRNA

Two siRNAs targeting ERK1/2 were designed by Shanghai GenePharma (Shanghai, China). The siRNA sequences used in the experiments were as follows: siERK-1 (sense, 5′-TGGCTTCTTGACGGAATATGTGG-3′), siERK-2(sense,5′-ACCTGAATTGTATCATCAACATG-3′). SiRNAs targeting ERK1/2 were used at a final concentration of 100 nM. Vero E6 cells and IPI-2I cells were transfected with the siRNAs or control siRNA using X-tremeGENE™ siRNA Transfection Reagent (Roche), according to the manufacturer's protocol. After transfection for 48 h, the cells were infected with SADS-CoV at a multiplicity of infection (MOI) of 0.1 for 36 h. The ERK1/2 proteins were detected with western blotting and the band intensities were quantified with densitometry using the ImageJ software. At 36 h postinfection (hpi), the infected cells were analyzed with western blotting, as described above. The culture supernatants were harvested and the virus within them titrated, as described below.

2.6. Virus titration

Vero E6 or IPI-2I cells were treated with each inhibitor or siRNA in duplicate, as described above. The culture supernatants were collected from the wells at different time points and stored at −80 °C. The SADS-CoV titer was measured in duplicate with limiting dilution on Vero E6 cells, as described previously (Zhang et al., 2020). Briefly, Vero E6 cells were cultured in 96-well plates to 90% confluence and infected with 10-fold serial dilutions of each supernatant. At 4–6 days postinfection, when the cytopathic effect had stabilized to a constant rate, the cells were analyzed with light microscopy. The median tissue culture infective dose ($TCID_{50}$)/mL was calculated with the Spearman–Kärber method.

2.7. Apoptosis assays

Vero E6 cells were pretreated with U0126 or dimethyl sulfoxide (DMSO) for 1 h and then mock infected or infected with SADS-CoV at an MOI of 0.1. The virus-inoculated cells were further propagated in the presence of U0126 or DMSO. Apoptosis was evaluated with an Annexin V–FITC/Propidium Iodide (PI) assay (BD Biosciences Pharmingen, CA, USA), according to the manufacturer's protocol. In brief, cells were harvested, washed with cold PBS, and resuspended in 1 × binding buffer. The cells were then stained with FITC–annexin V and PI for 15 min at room temperature in the dark and analyzed with flow cytometry (BD FACSCalibur, USA) within 1 h. Cells negative for PI uptake and positive for annexin V were considered apoptotic.

2.8. Cell viability assay

The cytotoxic effects of all the reagents used in this study were analyzed with the Cell Counting Kit-8 (CCK-8) system (Dojindo, Japan) to detect cell viability, according to the manufacturer's instructions. Briefly, Vero E6 or IPI-2I cells were grown at 1×10^4 cells/well in a 96-well tissue culture plate and treated with each chemical for 36 h. After incubation for 36 h, CCK-8 solution (10 μL per 100 μL of medium in each well) was added to each well. The plates were then incubated at 37 °C for 1 h, and the absorbance was read at a wavelength of 450 nm with an enzyme-linked immunosorbent assay plate reader. All CCK-8 assays were performed in triplicate.

2.9. Statistical analysis

Data are shown as the means ± standard deviations (SD) of three independent experiments performed in triplicate. The results were analyzed with one-way analysis of variance ANOVA. Differences with $P < 0.05$ were considered statistically significant.

3. Results

3.1. SADS-CoV infection activates ERK1/2 in Vero E6 and IPI-2I cells

To investigate the effect of SADS-CoV on the ERK1/2 signaling cascade, the kinetics of ERK1/2 phosphorylation were monitored with western blotting in Vero E6 and IPI-2I cells infected with SADS-CoV at different doses and at different times postinfection. As shown in Fig. 1A, only small amounts of activated ERK1/2 were detected in the mock-infected Vero E6 and IPI-2I cells, used as the negative controls. In contrast, SADS-CoV infection significantly stimulated ERK1/2 activity by 6 hpi, and was most strongly induced at 36 hpi. In addition, there was a virus dose-dependent increase of activated ERK1/2 in Vero cells but a dose-dependent decrease in IPI-21 cells (Fig. 1B). These results indicate that SADS-CoV infection triggers the strong but temporary activation of ERK1/2. Interestingly, a newly expressed viral protein was first evident at 24 hpi (Fig. 1A), whereas the maximal phosphorylation status of ERK1/2 was observed at 36 hpi, suggesting that ERK1/2 activation occurs independently of SADS-CoV replication. Because ERK1/2 phosphorylation did not increase steadily with ongoing viral replication, we assumed that ERK1/2 activation occurred independently of the considerable protein production obvious at later time points. To test this hypothesis, Vero E6 and IPI-2I cells were treated with equal amounts of UV-irradiated inactivated virus, which can bind to and invade the target cells, but is incapable of expressing viral genes (Fig. 1C). As shown in Fig. 1C, UV-inactivated virus sufficiently stimulated ERK1/2 activation, and the pattern and timing of phosphorylation ERK were different in the UV inactivated virus as compared with that of live virus treated cells (Fig. 1C vs. 1A). This phenomenon was also observed in some other viruses, such as PRRSV (Lee and Lee, 2010). These data suggest that the initial cell entry events of the SADS-CoV life cycle are responsible for monophasic ERK activation.

3.2. SADS-CoV causes p-ERK1/2 to translocate to the nucleus and phosphorylate ELK1

After stimulation, a large number of ERK molecules accumulate in the nucleus and activate a series of transcription factors. The subcellular localization of p-ERK1/2 was examined in cells infected with SADS-CoV (Fig. 2A). There was no significant ERK1/2 activity in the mock-infected cells during the entire experiment. However, in the SADS-CoV-infected cells, a punctate nuclear distribution of p-ERK1/2 was observed at 24 hpi and p-ERK1/2 was continuously detected in the nucleus by 48 hpi. A western blotting analysis of nuclear and cytoplasmic extracts from the Vero E6 cells showed significantly enhanced translocation of p-ERK1/2 into the nucleus upon infection (Fig. 2B). It is well known that phosphorylated ERK1/2 translocate from the cytoplasm to the nucleus, where they activate a variety of targets, including transcription factor ELK1. Because transcription factor ELK1 acts downstream from the ERK signaling pathway and its activity is regulated by its ERK-dependent phosphorylation (Shaul and Seger, 2007), we measured the activation status of ELK1 after cells were infected with SADS-CoV at different times (Fig. 2C). No active ELK1 was detected in the mock-infected cells. In contrast, SADS-CoV infection resulted in the phosphorylation of ELK1 with kinetics that identically paralleled those observed for ERK1/2 activation. These findings indicate that the ERK signal activated by SADS-CoV infection regulates downstream effector molecules that control the expression of target genes essential for inducing cellular processes.

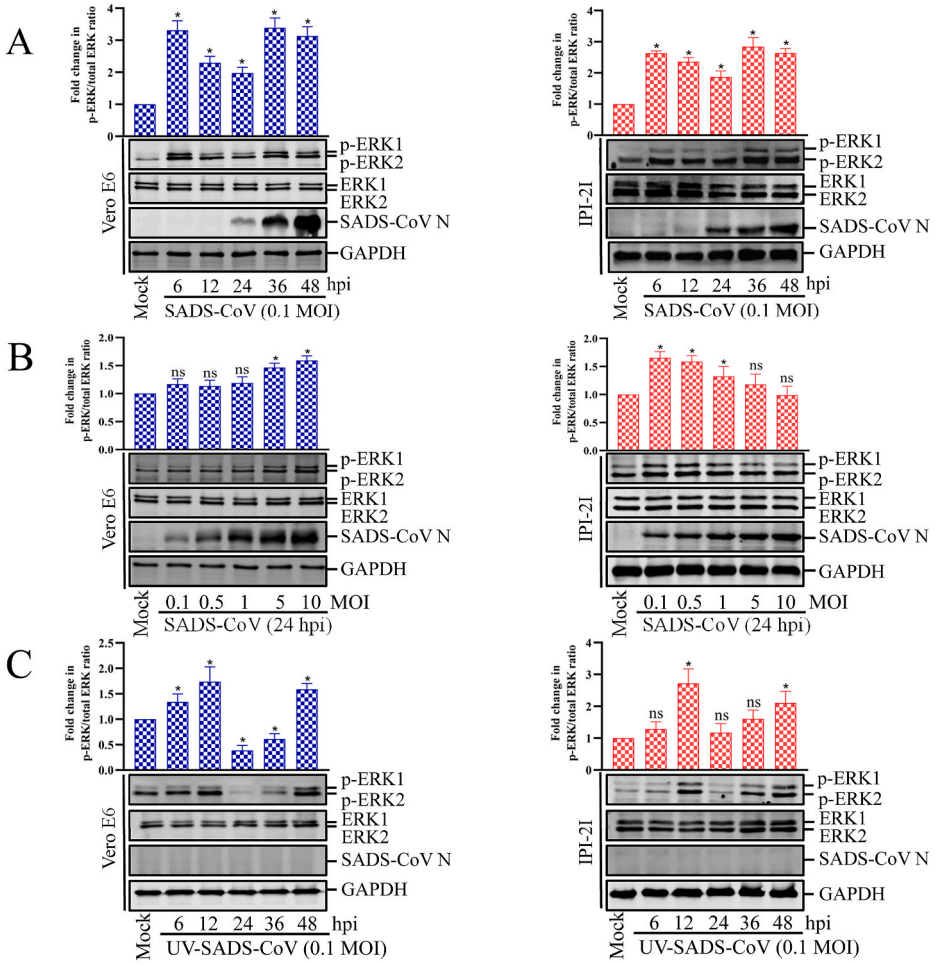

Fig. 1. SADS-CoV infection activates the ERK1/2 signaling pathway in cultured cells. (A and B) Vero E6 and IPI-2I cells were serum-starved for 24 h before mock infected or infected with SADS-CoV at MOI = 0.1 and at different times or at different MOIs at 24 hpi. Cells were cultured in DMEM with 0.25% trypsin during the whole SADS-CoV infection. (C) Vero E6 and IPI-2I cells were mock infected or infected with UV-SADS-CoV at MOI = 0.1 at different times. Western blotting analysis with an antibody specific for phosphorylated ERK1/2 (p-ERK1/2), ERK1/2, or SADS-CoV N protein. GAPDH was used as the internal loading control. Fold changes in the (p-ERK1/2)/(total ERK1/2) ratio are plotted. Results are representative means of three independent experiments, and error bars denote SD.

3.3. *ERK1/2 activation regulates SADS-CoV replication*

To examine the biological importance of ERK1/2 activation in SADS-CoV infection, experiments were performed with two specific inhibitors, U0126 and PD98059, which inhibit the activation of the SADS-CoV-induced ERK1/2 signaling pathway. The cytotoxicity of the ERK1/2 inhibitors for Vero E6 and IPI-2I cells was determined with a CCK-8 assay, and none of the tested U0126 or PD98059 doses caused any change in cell viability (Fig. 3A). Vero E6 cells were pretreated with various concentrations of the ERK1/2 inhibitor U0126 or PD98059 or with DMSO for 1 h and then infected with SADS-CoV at an MOI of 0.1. The inhibitors or DMSO were present during the entire period of infection. Virus production was confirmed with immunofluorescence and N protein expression at 36 hpi. The DMSO-treated control cells were positive for SADS-CoV N-protein-specific staining, confirming the infection and spread of the virus to neighboring cells (Fig. 3B). In contrast, U0126 and PD98059 clearly inhibited viral propagation. As shown in Fig. 3B, each inhibitor significantly and dose-dependently reduced SADS-CoV-induced viral gene expression. The quantification of N protein staining showed that the proportion (%) of virus-infected cells was similarly reduced during independent treatment with each inhibitor, which caused maximal (95%) inhibition at the highest concentration used (Fig. 3B). It is known that PD98059 prevents ERK1/2 activation by binding to unphosphorylated MEK1/2, the upstream activator of ERK1/2, whereas U0126 not only blocks the activation of MEK1/2, but also inhibits MEK1/2 activity (Davis et al., 2000). Therefore, U0126 is a more potent inhibitor of ERK1/2 activation than PD98059 (Favata et al., 1998). Our data also show that U0126 was significantly more effective in inhibiting SADS-CoV production than PD98059 at the same concentration. To examine the relevance of this phenomenon, the expression level of the SADS-CoV N protein in the presence of each inhibitor or DMSO was also evaluated with western blotting. As shown in Fig. 3C and D, the application of either inhibitor resulted in the downregulation of N protein expression at 36 hpi, accompanied by a significant reduction in the viral load in the cell culture supernatant compared with that of cells treated with DMSO (Fig. 3E and F). These findings indicate that the effect of each inhibitor on virus production correlates with the ability of each compound to inhibit ERK1/2 phosphorylation. Taken together, our data demonstrate that the ERK signaling pathway plays an important role in SADS-CoV replication.

To provide direct evidence of the involvement of the ERK cascade in the regulation of SADS-CoV, Vero E6 and IPI-2I cells were transfected with siRNA specific to ERK1/2 or with a commercial control nonspecific siRNA as the negative control. At 48 h posttransfection, the cells were infected with SADS-CoV, and the amounts of target gene expression and viral propagation were quantified at 36 hpi (Fig. 4A and B). The expression levels of the ERK molecules were reduced 0.63-fold in Vero E6 cells and 0.69-fold in IPI-2I cells after siERK-2 treatment compared to those in untreated cells or cells treated with the control siRNA, indicating the specific knockdown of ERK1/2 by the siRNA. As shown in Fig. 4A and B, the knockdown effect of siERK-2 was more obvious than that of siERK-1. Furthermore, the transfection of cells with ERK1/2-specific siRNA reduced the expression of the SADS-CoV N protein and the viral yield compared with those of the mock- or nonspecific-siRNA-transfected controls (Fig. 4C). These data show that the specific knockdown of ERK1/2 reduced viral propagation, demonstrating the essential role of ERK in SADS-CoV replication.

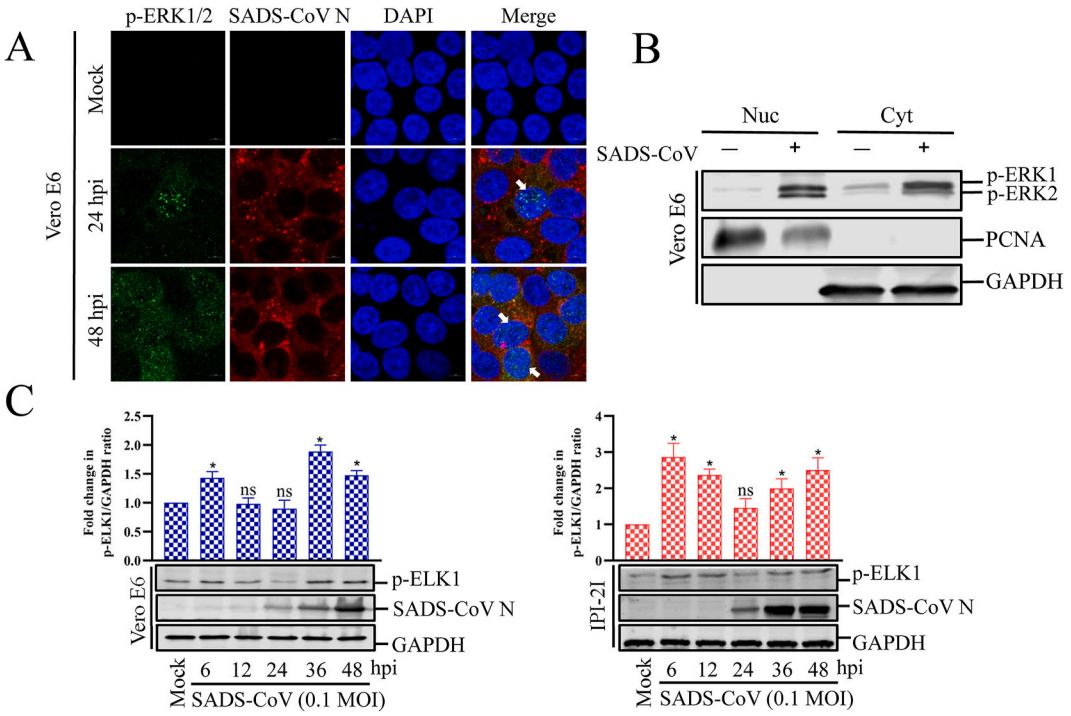

Fig. 2. SADS-CoV induces nuclear translocation of active ERK1/2 and phosphorylates ELK1. (A) SADS-CoV induces nuclear translocation of p-ERK1/2. Vero E6 cells were mock infected or infected with SADS-CoV at MOI = 0.1 at different times. Cells were fixed and costained with antibodies directed against p-ERK1/2 (green) and SADS-CoV N (red). The cells were then counterstained with DAPI and examined with a confocal laser scanning microscope (Zeiss). (B) Representative western blot of cytoplasmic and nuclear extracts of Vero E6 cells mock treated or infected with SADS-CoV for 36 h. GAPDH and PCNA reflect cytoplasmic and nuclear contents, respectively. (C) SADS-CoV induces ELK1 phosphorylation. Vero E6 and IPI-2I cells were mock infected or infected with SADS-CoV at MOI = 0.1 at different times. Western blotting analysis with antibody specific for phosphorylated ELK1 (p-ELK1) or SADS-CoV N protein. GAPDH was used as the internal loading control. Fold changes in the (p-ELK1)/(GAPDH) ratio are plotted. Results are representative means of three independent experiments, and error bars denote SD. (For interpretation of the references to colour in this figure legend, the reader is referred to the Web version of this article.)

3.4. Inhibition of ERK1/2 activation prevents SADS-CoV-mediated apoptosis

The RAF/MEK/ERK signaling pathway regulates numerous cellular processes, including apoptosis, autophagy, and senescence, *in vitro* and *in vivo* (Cagnol and Chambard, 2010). Growing evidence suggests that ERK activity is associated with classical markers of apoptosis, and promotes apoptotic cell death under certain conditions (Cagnol and Chambard, 2010). Interestingly, our previous studies indicates that the caspase-dependent FASL-mediated (extrinsic) and mitochondrion-mediated (intrinsic) apoptotic pathways play central roles in SADS-CoV-induced apoptosis, which facilitates viral replication (Zhang et al., 2020). Therefore, we speculated that the ERK pathway plays a role in the induction of apoptosis during SADS-CoV replication. To investigate whether ERK1/2 activation is required for SADS-CoV-induced apoptosis, the process of SADS-CoV-triggered apoptosis was assessed in the presence or absence of ERK inhibitor using annexin V/PI flow cytometry. Vero E6 cells were pretreated with 10 μM U0126, and the inhibitor was present during the entire period of infection. At 36 hpi, the treated and infected cells were stained with annexin V and PI and examined with fluorescence-activated cell sorting to quantitatively measure the percentages of viable, apoptotic, and dead cells. The results showed that the apoptosis of SADS-CoV-infected cells was significantly reduced at 36 hpi after treatment with U0126 (Fig. 5A). The expression levels of the SADS-CoV N protein in Vero E6 and IPI-2I cells in the presence of U0126 or DMSO were also evaluated with western blotting. As shown in Fig. 5B and C, 10 μM U0126 downregulated N protein expression at 36 hpi. When Vero E6 and IPI-2I cells infected with SADS-CoV were treated with 10 μM U0126, the SADS-CoV-induced cleavage of PARP was significantly reduced (Fig. 5B and C). The viral yield was also determined during treatment with U0126. After infection, the virus-containing supernatants were collected at 36 hpi and the viral titers were measured. As shown in Fig. 5D, the U0126 inhibitor suppressed the release of progeny virus at 36 hpi. Taken together, our data show that the ERK pathway is activated by SADS-CoV, and the chemical inhibition of this pathway negatively affects SADS-CoV-induced apoptotic cell death and viral replication, indicating that ERK pathway activity is required by this process.

4. Discussion

The importance of the interplay between host signaling pathways and various extracellular stimuli, including viral infection, has been reported (Fung and Liu, 2019; Gaur et al., 2011; Gupta et al., 2018). Among these transduction signals, the ERK cascade plays multiple significant roles in a variety of cellular functions that control cell fate. These, in turn, can regulate viruses, which rely entirely on the host cell machinery to survive (Cagnol and Chambard, 2010; Roux and Blenis, 2004). Therefore, viruses have evolved to regulate the ERK signaling of the host cell to benefit the viral replication machinery for optimal viral infection. However, no information is yet available on the intracellular signaling pathways involved in SADS-CoV replication. Here, for the first time, we have demonstrated that the ERK pathway is required for SADS-CoV-induced cellular apoptosis and the efficient replication of SADS-CoV in cultured cells. In this study, we have shown that SADS-CoV infection strongly induces the activation of the ERK pathway in Vero E6 and IPI-2I cells, suggesting a pivotal role for the ERK pathway in the early stage of SADS-CoV replication. Furthermore, the chemical inhibition or specific knockdown of ERK greatly impaired SADS-CoV propagation. We have also shown that the specific inhibition of ERK attenuates the SADS-CoV life cycle, evident as less viral protein and

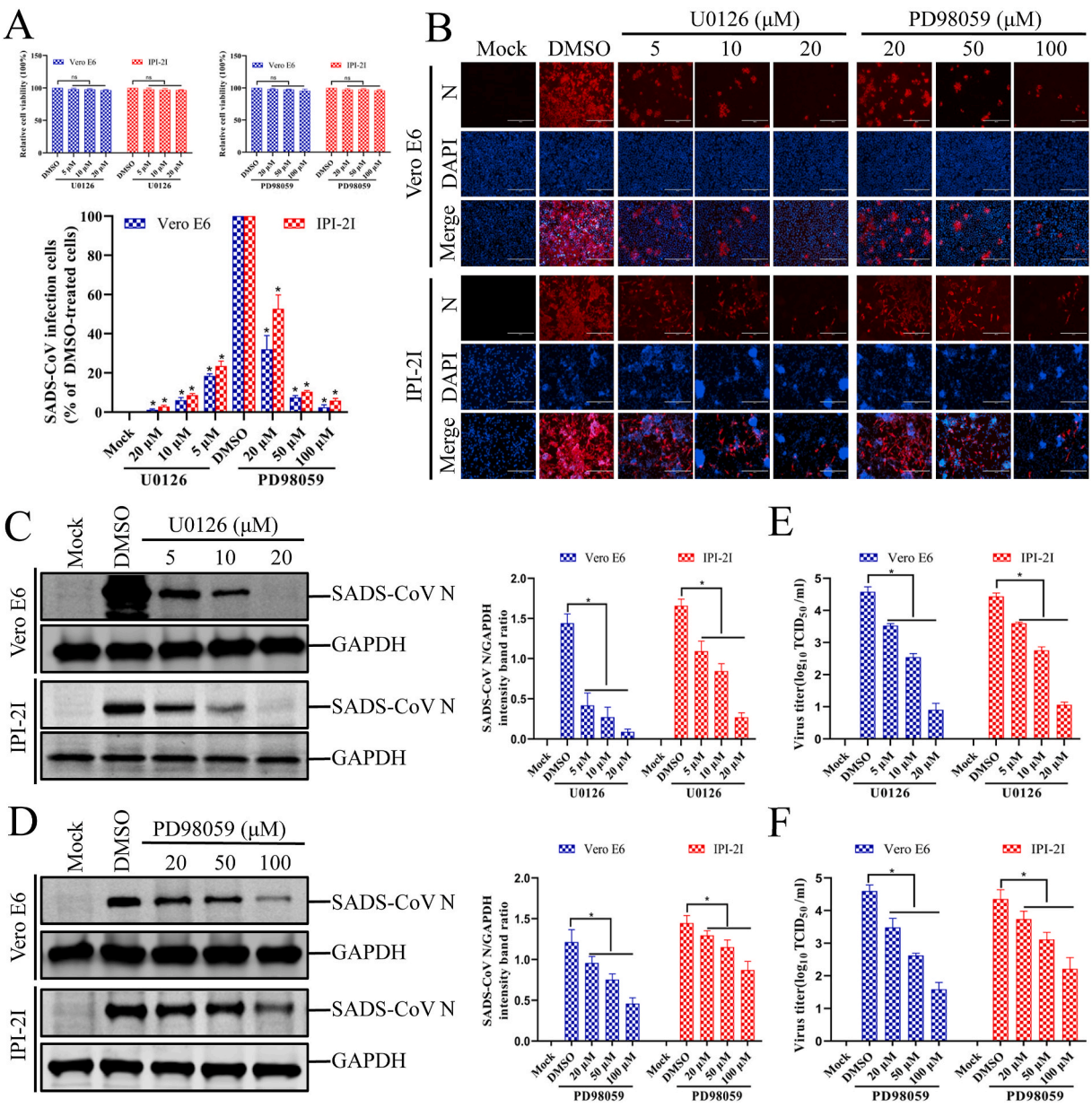

Fig. 3. Inhibition of ERK1/2 activation impairs SADS-CoV infection. (A) U0126 and PD98059 treatments do not affect cell viability. Vero E6 and IPI-2I cells were treated with U0126 or PD98059 at different concentrations or with the vehicle control DMSO for 36 h. Cell cytotoxicity was analyzed with the CCK-8 kit, as described in the Materials and Methods. (B) SADS-CoV propagation in the presence of U0126 or PD98059. Vero E6 cells were pretreated with either inhibitor at the indicated concentrations for 1 h and then infected with SADS-CoV. SADS-CoV-infected cells were further incubated for 36 h in the presence of DMSO, U0126, or PD98059. At 36 hpi, the virus-infected cells were subjected to an immunofluorescence assay with an anti-SADS-CoV-N antibody, followed by DAPI counterstaining and examination under an inverted fluorescence microscope. The percentage of SADS-CoV-infected cells per view is expressed as the mean ± SD of three independent experiments. (C and D) Viral N protein expression in the presence of U0126 or PD98059. Vero E6 and IPI-2I cells were treated with DMSO, U0126, or PD98059 at the indicated concentration for 1 h before infection with SADS-CoV. The SADS-CoV-infected cells were then incubated for a further 36 h in the presence of DMSO, U0126, or PD98059. At 36 hpi, the cell lysates were examined with western blotting, probed with an antibody directed against SADS-CoV N protein. The blot was also reacted with a mouse monoclonal antibody directed against GAPDH to verify equal protein loading. Densitometric data for SADS-CoV N/GAPDH are expressed as the means ± SD of three independent experiments. (E and F) U0126 or PD98059 treatment suppressed SADS-CoV replication. Treatment and infection conditions were as described for panels C and D. The viral titers in the supernatants collected at 36 hpi were determined with the Spearman–Kärber method. Error bars represent the standard errors of the means of three independent experiments.

progeny production, reduced viral cleavage of host proteins, and the attenuation of host cell death. This study provides new insights into the interplay between the virus and the host signaling induced by SADS-CoV infection, and demonstrates that ERK signaling is required for the pathogenesis of SADS-CoV.

The significance of the activation of host ERK has been demonstrated in other models of viral infection. In a Human immunodeficiency virus 1 (HIV-1) model, ERK activation benefited viral replication, and the inhibition of these phosphorylation events seemed to inhibit viral replication (Jacque et al., 1998). Similarly, the following viruses also interact with ERK1/2: Hepatitis C virus (Giambartolomei et al., 2001), Borna disease virus (Planz et al., 2001), Influenza A virus (Pleschka et al., 2001), and adenovirus type 7 (Alcorn et al., 2001). For other coronaviruses such as Porcine deltacoronavirus (PDCoV)、Porcine epidemic diarrhea virus (PEDV)、Middle East respiratory syndrome coronavirus (MERS-CoV), it also has proved that ERK was specifically

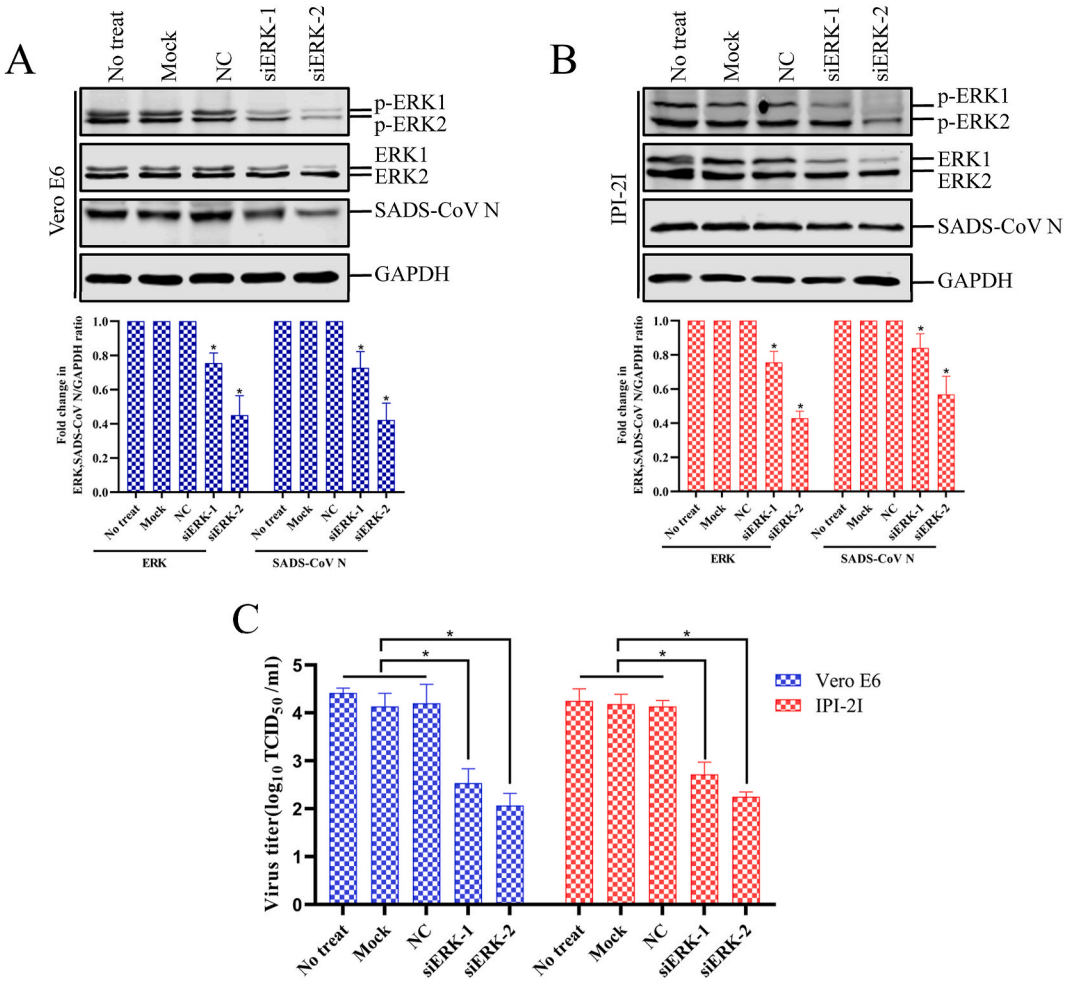

Fig. 4. Knockdown of ERK1/2 inhibits the replication of SADS-CoV. (A and B) Vero E6 and IPI-2I cells were untreated (No treat), treated with transfection reagent only (mock), treated with control siRNA (NC), treated with siERK-1 or siERK-2 for 48 h and then infected with SADS-CoV for 36 h. The cells were harvested and analyzed with western blotting with anti-p-ERK1/2, anti-ERK1/2, anti-viral N, or anti-GAPDH antibody. (C) The virus-containing supernatants were collected at 36 hpi and the viral titers calculated with the Spearman–Kärber method. Error bars represent the standard errors of the means of three independent experiments.

modulated in response to virus infection *in vitro* throughout the course of infection (Jeon et al., 2020; Kim and Lee, 2015; Kindrachuk et al., 2015). Such widespread ERK involvement suggests either that it constitutes a global viral strategy to enhance the viral replicative machinery or that ERK1/2 activation is a universal response of the host to protect against infection.

These observations were similarly reproduced in the porcine intestinal epithelial cell line IPI-2I infected with infectious or UV-inactivated SADS-CoV, indicating that SADS-CoV-induced ERK signaling is independent of the cell type. Interestingly, other nidoviruses trigger similar ERK1/2 activation kinetics in response to viral entry, suggesting that the ERK pathway has a unique role in nidovirus biology (Cai et al., 2007; Jeon et al., 2020; Kim and Lee, 2015; Lee and Lee, 2010). In other viruses, such as human gammaherpesvirus 8, coxsackievirus B3, and human astrovirus, the rapid transient activation of the ERK pathway is observed within 10–15 min of infection (Luo et al., 2002; Moser and Schultz-Cherry, 2008; Sharma-Walia et al., 2005). However, in the present study, the relatively slow growth rate of SADS-CoV meant we could not determine how quickly the ERK pathway is activated after infection. Although we did not identify the exact mechanism by which ERK signaling is induced by SADS-CoV infection, it may be mediated by direct virus–receptor binding, such as occurs during for HIV-induced ERK activation (Popik et al., 1998). However, we cannot exclude the activation of the ERK cascade by other stimuli, including by incoming viral particles through their direct fusion or by disassembled viral proteins and the released genome after the viral uncoating process.

The data presented here raise the question of the exact function of activated ERK during SADS-CoV infection. A reasonable explanation of how ERK regulates SADS-CoV infection is that the ERK pathway modulates viral replication directly or indirectly. In this study, two ERK inhibitors, PD98059 and U0126, were used to investigate how ERK signaling favors the replication of SADS-CoV. PD98059 prevents ERK activation by blocking the phosphorylation of ERK1/2, whereas U0126 not only inhibits the activation of ERK1/2 but also inhibits ERK1/2 activity (Alessi et al., 1995; Davis et al., 2000). The treatment of SADS-CoV-infected cells with PD98059 or U0126 significantly suppressed the individual postinternalization steps of the viral replication process, including protein expression and virus production. A similar result was observed in PEDV, another enteric swine coronavirus, where the two inhibitors independently inhibited ERK activation, potently impairing PEDV replication (Kim and Lee, 2015). However, in another coronavirus, Porcine deltacoronavirus (PDCoV), U0126 significantly and dose-dependently suppressed PDCoV gene expression, whereas PD98059 had no detrimental effect on PDCoV replication. This is because PD98059 does not affect PDCoV-induced ERK activation, whereas U0126 markedly reduces the levels of p-ERK1/2. Considering previous and current findings, the replication of SADS-CoV and PEDV seems to be more dependent on the magnitude of ERK activation than does the replication of PDCoV, indicating that the dependence of infection upon ERK differs among coronaviruses. At present, a variety of

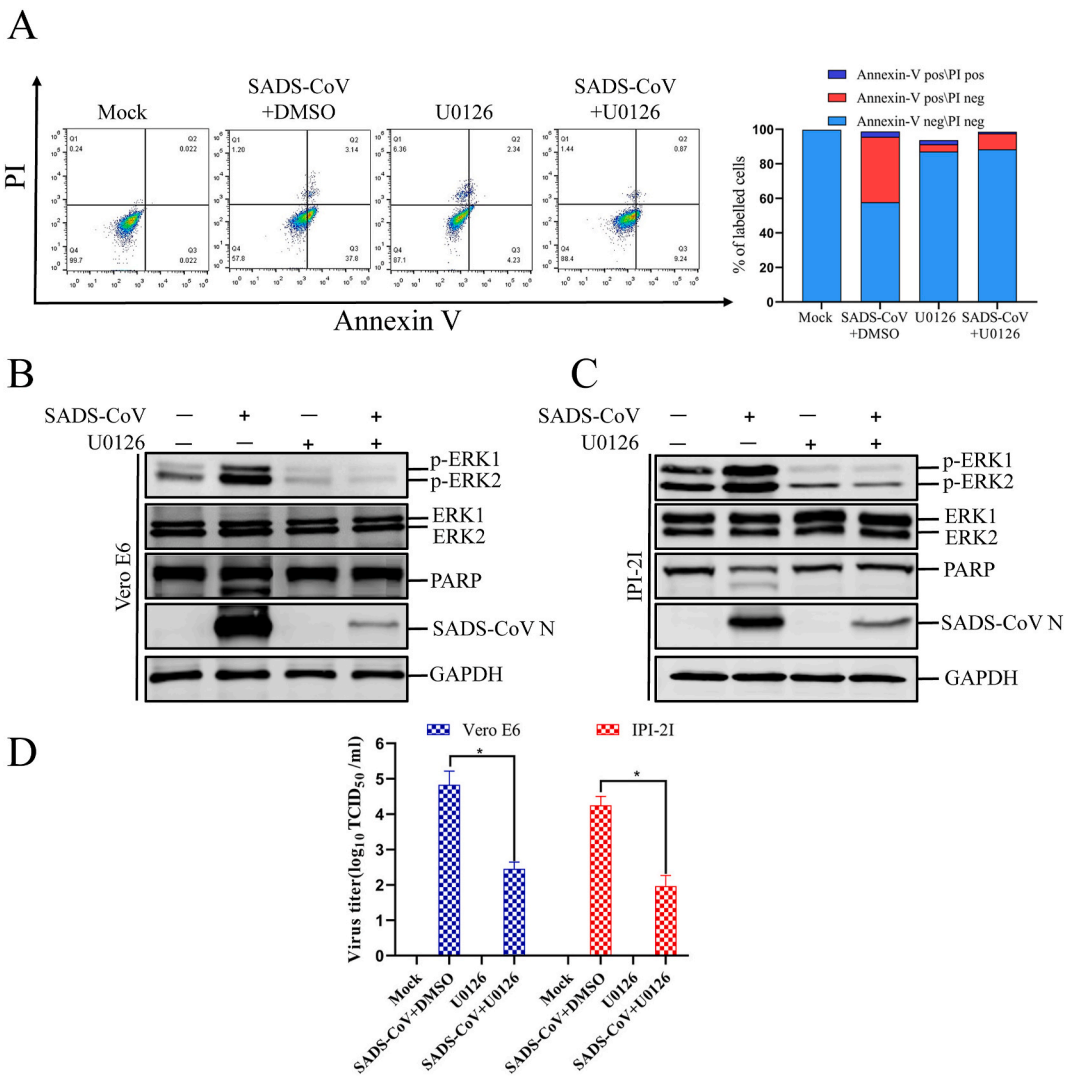

Fig. 5. U0126 blocks SADS-CoV-induced apoptosis. (A) Vero E6 cells were mock infected or infected with SADS-CoV (MOI = 0.1) in the presence or absence of U0126 (10 μM) for 36 h. They were washed twice with cold PBS and resuspended in 1 × binding buffer. The cells were stained with FITC–annexin V and PI for 15 min and analyzed with flow cytometry (BD FACSCalibur, USA) within 1 h. Q1: necrotic or other cell population, which was FITC–annexin V negative and PI positive; Q2: end-stage apoptotic or dead cell population, which was FITC–annexin V and PI positive; Q3: early apoptotic cell population, which was FITC–annexin V positive and PI negative; Q4: viable cell population that was not undergoing apoptosis, which was both FITC–annexin V and PI negative. The graph on the right represents the percentage of each cell population nonsignificant percentages of annexin-V-negative and PI-positive cells were excluded. (B and C) Vero E6 and IPI-2I cells were mock infected or infected with SADS-CoV at an MOI of 0.1 in the presence or absence of U0126 (10 μM). After incubation for 36 h, a western blotting analysis with antibody specific for p-ERK1/2, ERK1/2, PARP, or SADS-CoV N protein. GAPDH was used as the internal loading control. (D) The virus-containing supernatants were collected at 36 hpi and the viral titers were calculated with the Spearman–Kärber method. Error bars represent the standard errors of the means of three independent experiments.

antiviral strategies against coronaviruses based on virus infection mechanism have been reported, including receptor blockers and virus replicase inhibitors, which plays an important role in the development of antiviral drugs(Su et al., 2021). Considering the role of the ERK signaling pathway in the pathogenesis of various viruses, it is probable that define targets for antiviral therapy and design drugs that inhibit the ERK signaling pathway (Ghasemnejad-Berenji and Pashapour, 2021). Prior data had indicated that the hydroxychloroquine (HCQ) could influence the MAPK cascade to further against Severe Acute Respiratory Syndrome CoronaVirus 2 (SARS-CoV-2) infection(Mohanta et al., 2020). Targeted blocking of ERK pathways by designing small-molecule drugs based on the pathways of viral regulation of the cell apoptosis is an effective strategy of inhibiting viral replication.

The activation of the ERK pathway results in the phosphorylation of numerous ERK target proteins, which mediate multiple cellular functions. The ternary complex factor ELK1 is a prime nuclear substrate of the MAPKs c-Jun N-terminal protein kinase (JNK), p38, and ERK, which plays a pivotal role in apoptosis induction by various extracellular signals (Davis et al., 2000; Liu et al., 2019; Shao et al., 1998). ERK phosphorylation-dependent activation of ELK1 by binding some apoptosis-related molecules promotor regions mediated cell apoptosis, which could account for ELK1 controlling of cell proliferation and apoptosis (Yano et al., 2019).In the HIV-1 model, ERK activation enhanced viral infectivity and replication, possibly as the result of the direct phosphorylation of the viral protein Vif65. It is still unknown how SADS-CoV replication is regulated by the ERK signaling pathway. Perhaps this process involves the direct phosphorylation of intracellular components that are required for viral replication. Alternatively, ERK activity may be necessary to activate SADS-CoV proteins, such as the RNA-dependent RNA polymerases (RdRps), which are essential for the initiation of viral RNA replication. The RdRps of positive-sense RNA viruses are reported to be phosphoproteins activated by host proteins,

suggesting that viral RNA replication is regulated by the phosphorylation of the polymerase proteins (Jakubiec and Jupin, 2007). Previous studies have also suggested that ERK1/2 activity is necessary to phosphorylate or stabilize the viral RdRps, which are both required for the initiation of viral RNA replication (Luo et al., 2002). Therefore, similar phosphorylation modification may activate the SADS-CoV RdRp nsp12 and could be essential for optimal viral RNA synthesis.

ERK1/2 activation mediates apoptosis through either the intrinsic or extrinsic pathway by the induction of mitochondrial cytochrome *c* release or caspase 8 activation, respectively (Cagnol and Chambard, 2010). Several viruses have been shown to activate the ERK pathway to modulate apoptosis, facilitating to their replication (Wong et al., 2005; Zampieri et al., 2007). In our previous studies, we have shown that SADS-CoV induces apoptosis after infection, both *in vitro* and *in vivo*. We have also demonstrated that both the caspase-dependent FASL-mediated (extrinsic) and mitochondrion-mediated (intrinsic) apoptotic pathways play central roles in SADS-CoV-induced apoptosis, which then facilitates viral replication (Zhang et al., 2020). Interestingly, in this study, we have also shown a positive correlation between the activation of ERK1/2 and apoptosis during SADS-CoV infection. However, previous studies showed a negative correlation between the activation of ERK1/2 and apoptosis during PEDV infection (Kim and Lee, 2015) and PDCoV (Jeon et al., 2020) infection. The mechanism by which the inhibition of the ERK pathway prevents SADS-CoV-induced apoptosis is likely to be the indirect result of reduced viral replication and/or infectivity, analogous to the contribution of ERK to influenza virus infection (Pleschka et al., 2001). Although many studies have supported the general view that the activation of the ERK pathway delivers a survival signal that counteracts the proapoptotic effects associated with p38 MAPK and/or JNK activation (Xia et al., 1995), several studies have correlated ERK and the apoptotic cascade. For example, it has been reported that ERK activation is required for the cisplatin-induced apoptosis of HeLa cells and functions upstream from caspase activation to initiate the apoptotic signal (Wang et al., 2000). The overproduction of proto-oncogenes downstream from ERK, such as C-MYC may trigger apoptosis at the level of the mitochondrion (Soucie et al., 2001). Joe et al. (1996) have also shown that dominant inhibitory RAS delays Sindbis-virus-induced apoptosis in neuronal cells. The mechanism underlying the indirect induction of apoptosis by SADS-CoV replication and the possible contribution of direct host signaling events remain an important area of future research.

In summary, the findings presented here show that SADS-CoV infection activates ERK early in the infection of Vero E6 and IPI-2I cells and that ERK activation is required for efficient SADS-CoV replication *in vitro*. However, the exact viral processes and constituents responsible for ERK activation remain unknown. We also provide the first direct evidence that the ERK signaling pathway is a crucial cellular factor in mediating SADS-CoV-induced apoptosis. Therefore, the identification of the relevant apoptotic signaling pathway in mammalian cells will provide insight into the mechanisms by which SADS-CoV infection causes cell death. Further analysis of the pathways linking ERK to viral replication and cell apoptosis will provide strategies to control SADS-CoV gene expression and infection, and the associated diseases.

Data availability statement

All data generated or analyzed during this study are included in this article.

CRediT authorship contribution statement

Jiyu Zhang: Conceptualization, Methodology, Data curation, Formal analysis, Writing – original draft. **Liaoyuan Zhang:** Conceptualization, Methodology, Data curation, Formal analysis, Writing – original draft. **Hongyan Shi:** Conceptualization, Methodology, Formal analysis, Writing – review & editing. **Shufeng Feng:** Data curation, Formal analysis, Resources. **Tingshuai Feng:** Methodology, Data curation, Formal analysis. **Jianfei Chen:** Methodology, Data curation, Formal analysis. **Xin Zhang:** Methodology, Resources. **Yuru Han:** Methodology, Resources. **Jianbo Liu:** Methodology, Resources, Methodology. **Yiming Wang:** Resources. **Zhaoyang Ji:** Resources. **Zhaoyang Jing:** Resources. **Dakai Liu:** Methodology, Validation, Formal analysis. **Da Shi:** Investigation, Methodology, Project administration, Resources, Supervision, Visualization, Writing – original draft, Writing – review & editing. **Li Feng:** Conceptualization, Methodology, Project administration, Funding acquisition, Writing – review & editing.

Declaration of competing interest

The authors declare that they have no conflicts of interest.

Acknowledgements

This study was supported by the National Key Research and Development Program of China (2017YFD0500104 and 2017YFD0501603), the Heilongjiang Science Foundation Project (C2018066), and the Agricultural Science and Technology Innovation Program (CAAS-ZDRW202008).

References

Abe, M.K., Kuo, W.L., Hershenson, M.B., Rosner, M.R., 1999. Extracellular signal-regulated kinase 7 (ERK7), a novel ERK with a C-terminal domain that regulates its activity, its cellular localization, and cell growth. Mol. Cell Biol. 19, 1301–1312.

Alcorn, M.J., Booth, J.L., Coggeshall, K.M., Metcalf, J.P., 2001. Adenovirus type 7 induces interleukin-8 production via activation of extracellular regulated kinase 1/2. J. Virol. 75, 6450–6459.

Alessi, D.R., Cuenda, A., Cohen, P., Dudley, D.T., Saltiel, A.R., 1995. PD 098059 is a specific inhibitor of the activation of mitogen-activated protein kinase kinase in vitro and in vivo. J. Biol. Chem. 270, 27489–27494.

Bieniasz, P.D., 2004. Intrinsic immunity: a front-line defense against viral attack. Nat. Immunol. 5, 1109–1115.

Blenis, J., 1993. Signal transduction via the MAP kinases: proceed at your own RSK. Proc. Natl. Acad. Sci. U. S. A 90, 5889–5892.

Cagnol, S., Chambard, J.C., 2010. ERK and cell death: mechanisms of ERK-induced cell death–apoptosis, autophagy and senescence. FEBS J. 277, 2–21.

Cai, Y., Liu, Y., Zhang, X., 2007. Suppression of coronavirus replication by inhibition of the MEK signaling pathway. J. Virol. 81, 446–456.

Cohen, P., 1997. The search for physiological substrates of MAP and SAP kinases in mammalian cells. Trends Cell Biol. 7, 353–361.

Cui, J., Li, F., Shi, Z.L., 2019. Origin and evolution of pathogenic coronaviruses. Nat. Rev. Microbiol. 17, 181–192.

Davis, S., Vanhoutte, P., Pages, C., Caboche, J., Laroche, S., 2000. The MAPK/ERK cascade targets both Elk-1 and cAMP response element-binding protein to control long-term potentiation-dependent gene expression in the dentate gyrus in vivo. J. Neurosci. 20, 4563–4572.

Everett, R.D., Chelbi-Alix, M.K., 2007. PML and PML nuclear bodies: implications in antiviral defence. Biochimie 89, 819–830.

Favata, M.F., Horiuchi, K.Y., Manos, E.J., Daulerio, A.J., Stradley, D.A., Feeser, W.S., Van Dyk, D.E., Pitts, W.J., Earl, R.A., Hobbs, F., Copeland, R.A., Magolda, R.L., Scherle, P. A., Trzaskos, J.M., 1998. Identification of a novel inhibitor of mitogen-activated protein kinase kinase. J. Biol. Chem. 273, 18623–18632.

Fehr, A.R., Perlman, S., 2015. Coronaviruses: an overview of their replication and pathogenesis. Methods Mol. Biol. 1282, 1–23.

Fung, T.S., Liu, D.X., 2019. Human coronavirus: host-pathogen interaction. Annu. Rev. Microbiol. 73, 529–557.

Gaur, P., Munjhal, A., Lal, S.K., 2011. Influenza virus and cell signaling pathways. Med. Sci. Mon. Int. Med. J. Exp. Clin. Res. 17, RA148–154.

Ghasemnejad-Berenji, M., Pashapour, S., 2021. SARS-CoV-2 and the possible role of raf/MEK/ERK pathway in viral survival: is this a potential therapeutic strategy for COVID-19? Pharmacology 106, 119–122.

Giambartolomei, S., Covone, F., Levrero, M., Balsano, C., 2001. Sustained activation of the Raf/MEK/Erk pathway in response to EGF in stable cell lines expressing the Hepatitis C Virus (HCV) core protein. Oncogene 20, 2606–2610.

Gong, L., Li, J., Zhou, Q., Xu, Z., Chen, L., Zhang, Y., Xue, C., Wen, Z., Cao, Y., 2017. A new bat-HKU2-like coronavirus in swine, China, 2017. Emerg. Infect. Dis. 23.

Gupta, S., Kumar, P., Das, B.C., 2018. HPV: molecular pathways and targets. Curr. Probl. Cancer 42, 161–174.

Han, Y., Zhang, J., Shi, H., Zhou, L., Chen, J., Zhang, X., Liu, J., Wang, X., Ji, Z., Jing, Z., Cong, G., Ma, J., Shi, D., Li, F., 2019. Epitope mapping and cellular localization of swine acute diarrhea syndrome coronavirus nucleocapsid protein using a novel monoclonal antibody. Virus Res. 273, 197752.

Jacque, J.M., Mann, A., Enslen, H., Sharova, N., Brichacek, B., Davis, R.J., Stevenson, M., 1998. Modulation of HIV-1 infectivity by MAPK, a virion-associated kinase. EMBO J. 17, 2607–2618.
Jakubiec, A., Jupin, I., 2007. Regulation of positive-strand RNA virus replication: the emerging role of phosphorylation. Virus Res. 129, 73–79.
Jeon, J.H., Lee, Y.J., Lee, C., 2020. Porcine deltacoronavirus activates the Raf/MEK/ERK pathway to promote its replication. Virus Res. 283, 197961.
Joe, A.K., Ferrari, G., Jiang, H.H., Liang, X.H., Levine, B., 1996. Dominant inhibitory Ras delays Sindbis virus-induced apoptosis in neuronal cells. J. Virol. 70, 7744–7751.
Kim, Y., Lee, C., 2015. Extracellular signal-regulated kinase (ERK) activation is required for porcine epidemic diarrhea virus replication. Virology 484, 181–193.
Kindrachuk, J., Ork, B., Hart, B.J., Mazur, S., Holbrook, M.R., Frieman, M.B., Traynor, D., Johnson, R.F., Dyall, J., Kuhn, J.H., Olinger, G.G., Hensley, L.E., Jahrling, P.B., 2015. Antiviral potential of ERK/MAPK and PI3K/AKT/mTOR signaling modulation for Middle East respiratory syndrome coronavirus infection as identified by temporal kinome analysis. Antimicrob. Agents Chemother. 59, 1088–1099.
Lange-Carter, C.A., Pleiman, C.M., Gardner, A.M., Blumer, K.J., Johnson, G.L., 1993. A divergence in the MAP kinase regulatory network defined by MEK kinase and Raf. Science 260, 315–319.
Lechner, C., Zahalka, M.A., Giot, J.F., Moller, N.P., Ullrich, A., 1996. ERK6, a mitogen-activated protein kinase involved in C2C12 myoblast differentiation. Proc. Natl. Acad. Sci. U. S. A 93, 4355–4359.
Lee, J.D., Ulevitch, R.J., Han, J., 1995. Primary structure of BMK1: a new mammalian map kinase. Biochem. Biophys. Res. Commun. 213, 715–724.
Lee, Y.J., Lee, C., 2010. Porcine reproductive and respiratory syndrome virus replication is suppressed by inhibition of the extracellular signal-regulated kinase (ERK) signaling pathway. Virus Res. 152, 50–58.
Liu, Z., Liu, J., Ling, J., Yang, Q., Yang, H., Meng, P., Du, Q., Zhao, H.Q., Wang, Y.H., 2019. [Effects of ELK-1/JNK/c-Fos on apoptosis of rat hippocampal neurons cultured in vitro with Zuogui Jiangtang Jieyu Formula in simulated diabetes mellitus complicated with depression]. Zhongguo Ying Yong Sheng Li Xue Za Zhi 35, 50–54.
Luo, H., Yanagawa, B., Zhang, J., Luo, Z., Zhang, M., Esfandiarei, M., Carthy, C., Wilson, J.E., Yang, D., McManus, B.M., 2002. Coxsackievirus B3 replication is reduced by inhibition of the extracellular signal-regulated kinase (ERK) signaling pathway. J. Virol. 76, 3365–3373.
Mohanta, T.K., Sharma, N., Arina, P., Defilippi, P., 2020. Molecular insights into the MAPK cascade during viral infection: potential crosstalk between HCQ and HCQ analogues. Biomed Res Int 2020 8827752.
Moser, L.A., Schultz-Cherry, S., 2008. Suppression of astrovirus replication by an ERK1/2 inhibitor. J. Virol. 82, 7475–7482.
Planz, O., Pleschka, S., Ludwig, S., 2001. MEK-specific inhibitor U0126 blocks spread of Borna disease virus in cultured cells. J. Virol. 75, 4871–4877.
Pleschka, S., Wolff, T., Ehrhardt, C., Hobom, G., Planz, O., Rapp, U.R., Ludwig, S., 2001. Influenza virus propagation is impaired by inhibition of the Raf/MEK/ERK signalling cascade. Nat. Cell Biol. 3, 301–305.
Popik, W., Hesselgesser, J.E., Pitha, P.M., 1998. Binding of human immunodeficiency virus type 1 to CD4 and CXCR4 receptors differentially regulates expression of inflammatory genes and activates the MEK/ERK signaling pathway. J. Virol. 72, 6406–6413.
Randow, F., MacMicking, J.D., James, L.C., 2013. Cellular self-defense: how cell-autonomous immunity protects against pathogens. Science 340, 701–706.
Roux, P.P., Blenis, J., 2004. ERK and p38 MAPK-activated protein kinases: a family of protein kinases with diverse biological functions. Microbiol. Mol. Biol. Rev. : MMBR (Microbiol. Mol. Biol. Rev.) 68, 320–344.
Shao, N., Chai, Y., Cui, J.Q., Wang, N., Aysola, K., Reddy, E.S., Rao, V.N., 1998. Induction of apoptosis by Elk-1 and deltaElk-1 proteins. Oncogene 17, 527–532.
Sharma-Walia, N., Krishnan, H.H., Naranatt, P.P., Zeng, L., Smith, M.S., Chandran, B., 2005. ERK1/2 and MEK1/2 induced by Kaposi's sarcoma-associated herpesvirus (human herpesvirus 8) early during infection of target cells are essential for expression of viral genes and for establishment of infection. J. Virol. 79, 10308–10329.
Shaul, Y.D., Seger, R., 2007. The MEK/ERK cascade: from signaling specificity to diverse functions. Biochim. Biophys. Acta 1773, 1213–1226.
Soucie, E.L., Annis, M.G., Sedivy, J., Filmus, J., Leber, B., Andrews, D.W., Penn, L.Z., 2001. Myc potentiates apoptosis by stimulating Bax activity at the mitochondria. Mol. Cell Biol. 21, 4725–4736.
Su, M., Shi, D., Xing, X., Qi, S., Yang, D., Zhang, J., Han, Y., Zhu, Q., Sun, H., Wang, X., Wu, H., Wang, M., Wei, S., Li, C., Guo, D., Feng, L., Sun, D., 2021. Coronavirus porcine epidemic diarrhea virus nucleocapsid protein interacts with p53 to induce cell cycle arrest in S-phase and promotes viral replication. J. Virol. 95, e0018721.
Wang, X., Martindale, J.L., Holbrook, N.J., 2000. Requirement for ERK activation in cisplatin-induced apoptosis. J. Biol. Chem. 275, 39435–39443.
Wong, W.R., Chen, Y.Y., Yang, S.M., Chen, Y.L., Horng, J.T., 2005. Phosphorylation of PI3K/Akt and MAPK/ERK in an early entry step of enterovirus 71. Life Sci. 78, 82–90.
Xia, Z., Dickens, M., Raingeaud, J., Davis, R.J., Greenberg, M.E., 1995. Opposing effects of ERK and JNK-p38 MAP kinases on apoptosis. Science 270, 1326–1331.
Yano, S., Wu, S., Sakao, K., Hou, D.X., 2019. Involvement of ERK1/2-mediated ELK1/CHOP/DR5 pathway in 6-(methylsulfinyl)hexyl isothiocyanate-induced apoptosis of colorectal cancer cells. Biosci. Biotechnol. Biochem. 83, 960–969.
Zampieri, C.A., Fortin, J.F., Nolan, G.P., Nabel, G.J., 2007. The ERK mitogen-activated protein kinase pathway contributes to Ebola virus glycoprotein-induced cytotoxicity. J. Virol. 81, 1230–1240.
Zhang, J., Han, Y., Shi, H., Chen, J., Zhang, X., Wang, X., Zhou, L., Liu, J., Ji, Z., Jing, Z., Ma, J., Shi, D., Feng, L., 2020. Swine acute diarrhea syndrome coronavirus-induced apoptosis is caspase- and cyclophilin D- dependent. Emerg. Microb. Infect. 9, 439–456.
Zhou, P., Fan, H., Lan, T., Yang, X.L., Shi, W.F., Zhang, W., Zhu, Y., Zhang, Y.W., Xie, Q. M., Mani, S., Zheng, X.S., Li, B., Li, J.M., Guo, H., Pei, G.Q., An, X.P., Chen, J.W., Zhou, L., Mai, K.J., Wu, Z.X., Li, D., Anderson, D.E., Zhang, L.B., Li, S.Y., Mi, Z.Q., He, T.T., Cong, F., Guo, P.J., Huang, R., Luo, Y., Liu, X.L., Chen, J., Huang, Y., Sun, Q., Zhang, X.L., Wang, Y.Y., Xing, S.Z., Chen, Y.S., Sun, Y., Li, J., Daszak, P., Wang, L.F., Shi, Z.L., Tong, Y.G., Ma, J.Y., 2018. Fatal swine acute diarrhoea syndrome caused by an HKU2-related coronavirus of bat origin. Nature 556, 255–258.